RSC Advances

PAPER

View Article Online
View Journal | View Issue

Cite this: *RSC Adv.*, 2020, **10**, 12334

Solvent-assisted linker exchange as a tool for the design of mixed-linker MIL-140D structured MOFs for highly selective detection of gaseous H_2S†

Marcel Schulz, Nele Marquardt, Malte Schäfer, Thea Heinemeyer and Andreas Schaate *

Received 6th February 2020
Accepted 17th March 2020

DOI: 10.1039/d0ra01164a

rsc.li/rsc-advances

A MIL-140D-*sdc* framework has been used as a highly stable backbone for the introduction of 4,4′-azobenzene dicarboxylic acid (H_2*abdc*) *via* solvent-assisted ligand exchange (SALE). The implemented azo groups can serve as coordination sites for copper ions. These can exchange ligands with different gases, but show a high selectivity against H_2S, which makes this material promising for potential sensor applications.

Hydrogen sulfide (H_2S) is a toxic gas with harmful effects on human health and is responsible for different diseases, like liver cirrhosis.[1] At concentrations above just 50 ppm, irritation of the respiratory tract can occur.[2] For the detection of H_2S, chemical sensors containing semiconducting metal oxides are widely used. Although these exhibit high sensitivities, they also have some disadvantages due to their high working temperatures and a lack of selectivity.[3]

Especially in the areas of selectivity and cross-sensitivity, metal–organic frameworks (MOFs) can overcome the limits that plague many other sensors. Due to their modular design built up by metal nodes and organic linker molecules, they can be tailored to the desired application.[4] Functionalities attached to the linkers of MOFs are often required in order to be able to use these materials for sensor applications.[5]

Many MOFs are described for the detection of H_2S. Apart from one example of a capacitive sensor,[6] the detection is almost always based on a fluorescence turn-on probe. Here functional groups of the MOF ($-N_3$ or $-NO_2$) are reduced by H_2S to amino groups resulting in turning on the fluorescence of the linker. However, in these investigations the MOFs are dispersed in buffered aqueous or ethanolic solutions.[7] In addition, no gaseous H_2S is used, but sulfides-containing sodium salts such as Na_2S, that dissociate in solution to HS^-, which is required for the reaction.[8] To the best of our knowledge, only one example is described in literature where a MOF is used for a luminescent-based detection of gaseous H_2S.[9]

Azo components have the special ability to coordinate metal ions. This has already been investigated in detail with individual azo compounds and metal salts of palladium[10] or copper.[11,12] Until now, a transfer of this reaction behaviour into a MOF is rare and not yet described for copper species but for palladium species.[13] Nevertheless, these copper-azo complexes can be used for the colourimetric detection of both aqueous HS^- and gaseous H_2S.[14] The sensor principle is based on a displacement reaction. The coordinated copper ions react with gaseous H_2S to CuS as already shown with CuO-loaded metal oxide semiconductors.[15] Considering copper-based MOFs such as the HKUST-1, they show a lack of stability under normal conditions, making them unsuitable for use in sensor technology. Nevertheless, a reaction between H_2S and the metal centres is still possible, however, this leads to the formation of CuS and the complete breakdown of the framework.[16]

With the UiO family, a isoreticular series of Zr-based MOFs was reported.[17] Particularly, the UiO-66 and its derivatives exhibit an exceptional thermal and chemical stability. By the use of the same precursors but higher synthesis temperatures, Guillerm *et al.* presented highly stable Zr-MOFs, the so-called MIL-140 series.[18] In MIL-140 frameworks, there are one-dimensional chains of zirconium oxide (*c.n.* 7) as inorganic building units (IBUs) orientated parallel to the *c*-axis of the structures. Each chain is connected *via* linker molecules to six other chains resulting in a one-dimensional pore system (see ESI Fig. S1†). Especially those MOFs with longer linker molecules exhibit an improved stability in comparison to their UiO analogues. This can be explained with the different structures of these compounds.[18,19]

By using post-synthetic modifications (PSM) further functionalized MOF materials can be obtained.[20] In case of exchanging an unfunctionalized linker molecule with a functionalized, the solvent-assisted ligand exchange (SALE) is an attractive possibility to adjust the properties of an already synthesized MOF and enhance the tunability.[21]

Institute for Inorganic Chemistry, ZFM – Center for Solid State Chemistry and New Materials, Leibniz Universität, Callinstr. 9, 30167 Hannover, Germany. E-mail: andreas.schaate@acb.uni-hannover.de

† Electronic supplementary information (ESI) available. See DOI: 10.1039/d0ra01164a

We recently reported a low-temperature synthesis of MIL-140 frameworks and a new MIL-140-structured MOF, based on 4,4′-stilbenedicarboxylic acid (H_2*sdc*), the MIL-140D-*sdc* (see Table S1 and ESI Fig. S1†).[22] This MOF shows a high thermal and chemical stability which can be compared to the former reported MIL-140 MOFs.[18] A synthesis for an azo-based MIL-140D-*H* with H_2*abdc* as linker is also described in literature (see ESI Table S1†).[23] However, the resulting framework is instable under ambient conditions and a transition to a unknown nearly nonporous phase occurs after only a few days.[23] These are unfavourable properties for a stable sensor material.

In this work, we demonstrate the efficiency of the SALE to produce MOFs that combine high stability and high functionality. Therefore, we use the MIL-140D-*sdc* framework as stable backbone. For the preparation of the *mixed-linker* MOF (MIL-140D-*sdc*/*abdc*), we substitute sdc^{2-} with $abdc^{2-}$ *via* SALE by immersing the MIL-140D-*sdc* in a DMF solution of H_2*abdc* and storing it at 120 °C for 24 h (up to 1 eq. H_2*abdc* with respect to the Zr cations in the framework, see ESI Table S2†).

For verifying the successful SALE, the exchanged MOF samples were disassembled and analysed with ^{1}H-NMR spectroscopy (ESI Fig. S2 and S3†). The evaluation has shown that the level of conversion rises with an increasing amount of provided linkers (H_2*abdc*). The maximum exchange rate is slightly below 50%.

Powder X-ray diffraction (PXRD) is used to check the stability of the compounds after each reaction step. After exchanging the MIL-140D-*sdc* with $abdc^{2-}$ at 120 °C, the solids exhibit the same diffraction pattern, but the colour has changed from white to reddish (Fig. 1a).

The advantage of MIL-140 structured MOFs results from the stacking of the linkers and the resulting short distance between the azo groups. This arrangement should be promising for the coordination of copper ions, since in literature the molecules either have additional functional groups for the coordination or the metal ions are located between two azo groups.[24] Subsequently, copper ions are incorporated into the framework. For this purpose, the linker-exchanged MOF is dispersed in DMF and stirred for 1 hour at room temperature while adding copper chloride. The amount of copper chloride used is identical to the previously used amount of added linker H_2*abdc* (see ESI Table S3†). After the copper ions were integrated into the framework, the colour of the MOF changed from red to green (Fig. 1b). Although the samples still show the same diffraction pattern, a closer look reveals differences. Thus, the 200-reflection (at 5° 2Θ) shifts slightly to smaller angles and in the range of 10° 2Θ the intensity of two reflections increase (ESI Fig. S4†). Neither the shifted reflection nor the colour change can be observed during the treatment of UiO-*abdc* and MIL-140D-*H* with copper chloride. Additionally, pure MIL-140D-*H* appears not to be stable during this reaction (ESI Fig. S5 and S6†).

Nitrogen physisorption measurements verified that there is no significant quantity of linker molecules in the tunnel-like pores after the SALE (ESI Fig. S12 and Table S5†). In order to demonstrate that the integrated copper ions do not inhibit the accessibility of the pores, N_2 physisorption measurements have been repeated (ESI Fig. S13†). Indeed, the experimental BET areas barely change and are only about 100 $m^2\ g^{-1}$ lower (ESI Table S6†). It can therefore be assumed that the copper ions are coordinated at the azo groups of the linkers and thus hardly contribute to a loss of surface area.

For further simplification, at this point the focus is on the samples with the highest exchanged amount of linker and highest stored quantity of Cu^{2+} (1 eq. each). For a more detailed evaluation of the pore size and thus the location of the incorporated copper ions, argon physisorption measurements were carried out. Compared to the originally used sample MIL-140D-*sdc*, the BET areas are only slightly reduced and also the calculated pore size distributions for all samples show a good correlation (Fig. S15, S16 and Table S8†). Both measurements

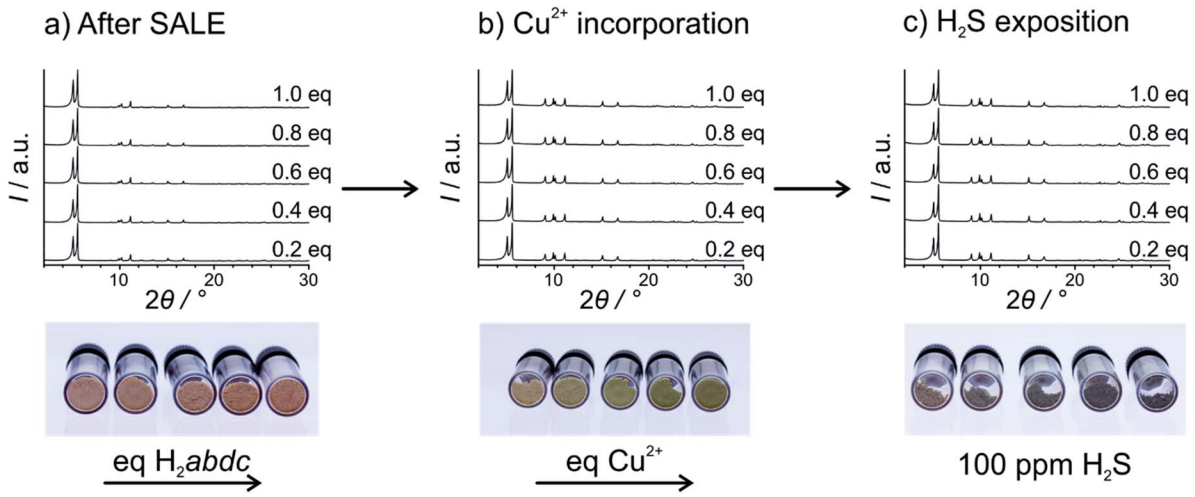

Fig. 1 Presentation of the conducted modification, incorporation and gas exposure with MIL-140D-*sdc* structured MOFs. (a) Powder XRD pattern of the samples prepared with a SALE starting from MIL-140D-*sdc* and the resulting colour change with different amounts of H_2*abdc*. (b) Powder XRD pattern after the incorporation of increasing amounts of Cu^{2+} into the MIL-140D-*sdc*/*abdc* framework and the observed colour change and (c) powder XRD pattern and pictures of the same materials after the exposure to 100 ppm H_2S.

indicate a coordination of the copper ions at the azo groups of the linkers. Furthermore, this result contradicts an excessive adsorption of the copper ions in the tunnel-like pores.

The amount of copper coordinated in the MOF is estimated by EDX spectroscopy. For this purpose, the MOF was offered two different quantities of copper salt (0.5 and 1.0 eq.) for complexation. In comparison to the SALE sample, the EDX measurements show the same copper content of 0.4 copper atoms per sum formula, regardless of whether 0.5 or 1.0 eq. copper salt was added (see ESI Fig. S17–S19 and Table S9†). The similar value is due to the fact that only half of the linkers are exchanged during the SALE and again suggests the coordination of the copper ions at the azo groups.

The thermogravimetric data are a further indication for the successful storage of Cu^{2+} in the framework. The sample obtained after the SALE shows a similar thermal decomposition as the starting material MIL-140D-*sdc*. Both materials have a thermal stability of about 350 °C, but the residual mass is lower than calculated in case of the SALE sample (ESI Fig. S21 and Table S10†). After incorporation, the residual mass increases by approximately 4.5*m*%, which is equivalent to a copper amount of approximately 0.45 per sum formula and in good agreement with the EDX spectroscopy. The reflections of the powder diffraction pattern of the residue can be accurately assigned to ZrO_2 and CuO (see ESI Fig. S7†). In addition, the percentage of guests in the framework is increasing drastically. This could be an indication that the copper ions act as Lewis acidic sites where solvent molecules preferentially coordinate. In order to estimate the Lewis acidity of a MOF, the shift of the acetone absorption band can be considered.[25] In the presence of strongly Lewis-acidic MOFs, the stretching vibration of the carbonyl group shifts to smaller wave numbers. In this case, the acetone vibration is located at 1690 cm^{-1} and thus 25 cm^{-1} lower than for uncoordinated acetone (see ESI Fig. S10†).

In the last step, the incorporated Cu^{2+} ions will be used for the detection of H_2S. With this approach it is possible to transfer the properties of the molecular complexes[11] into a solid state material, as we have already shown with a calixarene-based MOF for highly selective NO_2 detection.[26] It is generally assumed that the implicit chemical reaction is the formation of CuS.[15] Upon this reaction, a fast and impressive colour change occurs from green to black which can be simply observed with the naked eye. Taking the diffraction patterns into account, it is noticeable that the above-mentioned shift of the 200-reflection is reversed upon H_2S exposure, indicating a change in the coordination of the copper ions (see Fig. 1c and ESI Fig. S4†). After the exposure to H_2S, the BET area of all samples is drastically reduced (see ESI Fig. S14 and Table S7†) which can be explained by pore blocking effects due to CuS formation.

The formation of CuS can additionally be verified with Raman spectroscopy. Here, a weak CuS band can be found at 471 cm^{-1} (see ESI Fig. S11†). Again, this is an indication for the formation of CuS located inside the pore channels or on the surface of the MOFs as pore blocker. This is also an explanation for the decrease of the BET surfaces from the physisorption measurements. After the MOF has been exposed to H_2S, the acetone vibration disappears completely from the IR spectrum. This observation supports the thesis that the coordination of the copper ions at the azo groups and thus the Lewis acidic effect is no longer present after this step.

Additionally, the experimental residue of the MOF is similar to the Cu^{2+} incorporated sample (see ESI Fig. S21 and Table S10†) and is composed of ZrO_2 and CuO (see ESI Fig. S8†). Moreover, the EDX measurement show a sulphur content in this sample which is comparable to the amount of copper and obviously CuS is formed (see ESI Fig. S20 and Table S9†).

The chemical reaction of the sensor response is the formation of CuS and the associated colour change from green to black. For the application as H_2S sensor material, the spectroscopic characteristics were determined. As already can be seen in the photographs in Fig. 1, the colouration becomes more pronounced with increasing amount of provided linker during the SALE and thus also of the amount of incorporated Cu^{2+}. This observation is supported by the UV/Vis measurements. Here, the absorption also intensifies with increasing amounts of H_2*abdc* after the SALE in the range between 430 and 500 nm. The pure MIL-140D-*sdc* shows no absorption in this region at all (see ESI Fig. S22a†). The integration of azo groups is essential for the incorporation of copper ions into the MOF and thus for the detection of H_2S. When a pure MIL-140D-*sdc* is immersed in a copper chloride solution it can be shown that no copper is coordinated by the MOFs by comparison of the UV/Vis spectra. The absorption does not change because no copper ions can be complexed by the sdc^{2-} linker of pure MIL-140D-*sdc*. When the copper treated MIL-140D-*sdc* was exposed for 30 minutes to 100 ppm H_2S no measurable difference in the spectra occurs (see Fig. S24†). As a result, it can be concluded that no copper ions were deposited in the framework at all.

After the incorporation of copper ions in the MIL-140D-*sdc*/*abdc*, a second absorption maximum at 730 nm is visible (see ESI Fig. S22b†). As before, the maximum absorption increases with the amount of copper salt used. After exposure to H_2S, all samples immediately change their colour, whereby the highest absorption can be observed in the sample with the highest copper and $abdc^{2-}$ content. At this point, the entire absorption in the visible range of the light spectrum increases (see ESI Fig. S22c and S23†).

During a 30 minute exposure to 100 ppm H_2S a cycled UV/Vis measurement was conducted to observe directly the change in the absorbance. Within less than 1 minute, an increase of the absorption between 550 and 600 nm is visible. After 30 minutes the saturation is reached and absorbance is approximately 450 percent higher compared to the starting material after the Cu^{2+} incorporation (see Fig. 2). For a more precise analysis, the sample was exposed to 100 ppm H_2S for 30 minutes and the absorbance at 580 nm was recorded every five seconds. Here the MOF exhibits almost no absorption after the incorporation of Cu^{2+}. After the exposure to H_2S, the absorbance increases immediately and is again reaching a saturation point with an absorbance twice as high (see Fig. 3).

The next step was to investigate the selectivity. For this purpose, the MOF was exposed to various gases such as CO_2 and CO (100 ppm), NO_2 (10 ppm) or stored in an NH_3 and diethyl ether (DEE) atmosphere for 30 minutes. In terms of stability,

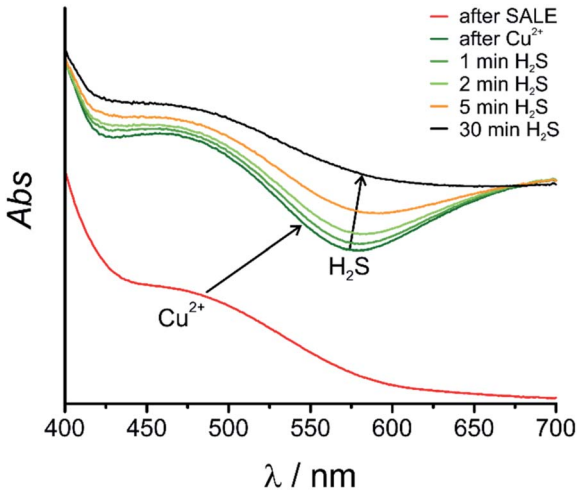

Fig. 2 UV/Vis spectra of the MIL-140D-*sdc*/*abdc* after the SALE with H_2*abdc* (red), after the incorporation of Cu^{2+} (green) and after the exposure to 100 ppm H_2S with different time steps ranging from 1 to 30 minutes.

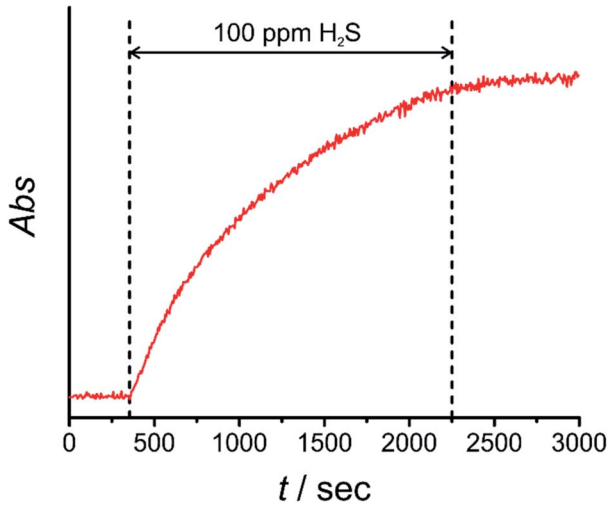

Fig. 3 UV/Vis measurement of the Cu^{2+} incorporated sample (1 eq.) at 580 nm. Before the gas exposure (100 ppm H_2S) a baseline was measured under room conditions.

a partly decomposition occurs only in presence of CO due to its interaction with the azo group (see ESI Fig. S9†).[27] Furthermore, the exposure to these gases results in a colour change for each sample, which can be explained by a ligand exchange at the coordinated copper ions (ESI Fig. S25†).[28] Each sample was again investigated with UV/Vis spectroscopy and the main differences in the spectra are in the range of 400 to 550 and 650 to 800 nm (see ESI Fig. S26†).

The other examined gases cause only minor changes in the range of 580 nm. Only in the case of H_2S a significant change in the spectrum at this wavelength was observed, which should enable quantitative detection of this gas. The absorbances of the different samples at 580 nm are compared and set in relation to the original absorbance of the copper stored sample. The

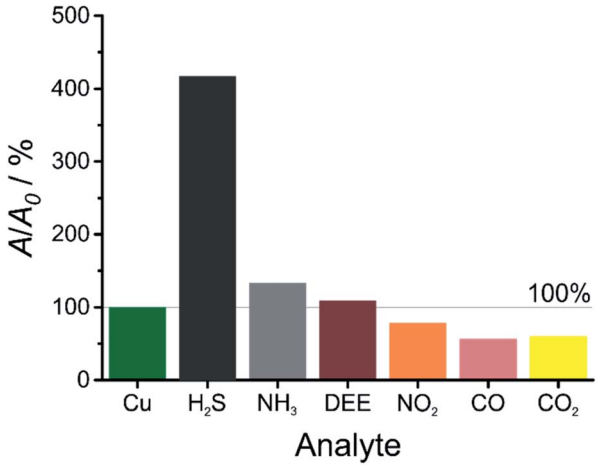

Fig. 4 Comparison of the differences in the absorbance of the sensor material in the presence of different gases (exposure time: 30 minutes). The measured values are all given in relation to the starting material whose absorbance was defined as 100%.

result is shown in Fig. 4, which demonstrates the high selectivity of this material for H_2S measured under these conditions.

In summary, it was demonstrated that through the post-synthetic step of the SALE a mixed-linker MOF has been obtained, the composition of which can be controlled by the amount of H_2*abdc* used in the SALE process. Furthermore, the new MIL-140D-*sdc*/*abdc* combines the stability of the MIL-140D-*sdc* framework and the functionality of the introduced azo groups. This again emphasizes the unique nature of the SALE for the production of differently functionalized frameworks and increases the tunability of manufactured materials. For the first time it was possible to use these linkers in a porous solid as coordination sites for copper ions. The porosity of the MOF is barely affected, making the coordinated metal ions accessible to guests. The guests can be different gases that coordinate under a ligand exchange with the copper ions. Nevertheless, this material has a high selectivity towards H_2S, which is expressed by the colour change from green to black, most likely due to the formation of CuS.

The MIL-140D-*sdc*/*abdc* seems to be an interesting starting material for the coordination of various metals, due to the close arrangement of the linkers. Further, more elaborated, functional groups could help to optimize the sensing process or enhance the reversibility of the sensing reaction. This property can be used for further post-synthetic modifications of the linker and might also result in other attractive sensor materials.

Conflicts of interest

There are no conflicts of interest to declare.

Acknowledgements

Fruitful discussions as well as general and financial support by Prof. Dr Peter Behrens are gratefully acknowledged.

Notes and references

1 (*a*) R. J. Reiffenstein, W. C. Hulbert and S. H. Roth, *Annu. Rev. Pharmacol. Toxicol.*, 1992, **34**, 109; (*b*) S. Fiorucci, E. Antonelli, A. Mencarelli, S. Orlandi, B. Renga, G. Rizzo, E. Distrutti, V. Shah and A. Morelli, *Hepatology*, 2005, **42**, 539–548.

2 T. L. Guidotti, *Occup. Med.*, 1996, **46**, 367–371.

3 (*a*) N. Joshi, T. Hayasaka, Y. Liu, H. Liu, O. N. Oliveira and L. Lin, *Microchim. Acta*, 2018, **185**, 213; (*b*) H.-J. Kim and J.-H. Lee, *Sens. Actuators, B*, 2014, **192**, 607–627; (*c*) I. Marr and R. Moos, *Sens. Actuators, B*, 2017, **248**, 848–855; (*d*) V. E. Bochenkov and G. B. Sergeev, in *Metal oxide nanostructures and their applications*, ed. A. Umar and Y.-B. Hahn, American Scientific Publ, Los Angeles, Calif., 2010, vol. 3, pp. 31–52.

4 (*a*) L. E. Kreno, K. Leong, O. K. Farha, M. Allendorf, R. P. van Duyne and J. T. Hupp, *Chem. Rev.*, 2012, **112**, 1105–1125; (*b*) M. J. Katz, J. E. Mondloch, R. K. Totten, J. K. Park, S. T. Nguyen, O. K. Farha and J. T. Hupp, *Angew. Chem.*, 2014, **126**, 507–511; (*c*) D. Farrusseng, S. Aguado and C. Pinel, *Angew. Chem., Int. Ed.*, 2009, **48**, 7502–7513; (*d*) H. Bux, A. Feldhoff, J. Cravillon, M. Wiebcke, Y.-S. Li and J. Caro, *Chem. Mater.*, 2011, **23**, 2262–2269.

5 A. Karmakar, P. Samanta, A. V. Desai and S. K. Ghosh, *Acc. Chem. Res.*, 2017, **50**, 2457–2469.

6 O. Yassine, O. Shekhah, A. H. Assen, Y. Belmabkhout, K. N. Salama and M. Eddaoudi, *Angew. Chem., Int. Ed.*, 2016, **55**, 15879–15883.

7 (*a*) X. Zhang, J. Zhang, Q. Hu, Y. Cui, Y. Yang and G. Qian, *Appl. Surf. Sci.*, 2015, **355**, 814–819; (*b*) S. S. Nagarkar, T. Saha, A. V. Desai, P. Talukdar and S. K. Ghosh, *Sci. Rep.*, 2014, **4**, 7053.

8 H. A. Henthorn and M. D. Pluth, *J. Am. Chem. Soc.*, 2015, **137**, 15330–15336.

9 J. Zhang, F. Liu, J. Gan, Y. Cui, B. Li, Y. Yang and G. Qian, *Sci. China Mater.*, 2019, **62**, 1445–1453.

10 (*a*) M. Ghedini, I. Aiello, A. Crispini, A. Golemme, M. La Deda and D. Pucci, *Coord. Chem. Rev.*, 2006, **250**, 1373–1390; (*b*) A. Bjelopetrović, S. Lukin, I. Halasz, K. Užarević, I. Đilović, D. Barišić, A. Budimir, M. Juribašić Kulcsár and M. Ćurić, *Chem.–Eur. J.*, 2018, **24**, 10672–10682; (*c*) D. Babić, M. Ćurić and D. M. Smith, *J. Organomet. Chem.*, 2011, **696**, 661–669.

11 W.-B. Yu, Q.-Y. He, X.-F. Ma, H.-T. Shi and X. Wei, *Dalton Trans.*, 2015, **44**, 351–358.

12 (*a*) M. S. Masoud, E. A. Khalil, A. M. Hindawy, A. E. Ali and E. F. Mohamed, *Spectrochim. Acta, Part A*, 2004, **60**, 2807–2817; (*b*) S. M. Abdallah, *Arabian J. Chem.*, 2012, **5**, 251–256; (*c*) R. Gup, E. Giziroglu and B. Kırkan, *Dyes Pigm.*, 2007, **73**, 40–46.

13 H. V. Le, Q. T. T. Nguyen, T. T. Co, P. K. T. Nguyen and H. T. Nguyen, *J. Electron. Mater.*, 2018, **47**, 6918–6922.

14 (*a*) L. Engel, K. R. Tarantik, C. Pannek and J. Wöllenstein, *Sensors*, 2019, **19**, 1189; (*b*) D. Zhang and W. Jin, *Spectrochim. Acta, Part A*, 2012, **90**, 35–39.

15 T. Maekawa, J. Tamaki, N. Miura and N. Yamazoe, *Chem. Lett.*, 1991, **20**, 575–578.

16 J. Ethiraj, F. Bonino, C. Lamberti and S. Bordiga, *Microporous Mesoporous Mater.*, 2015, **207**, 90–94.

17 J. H. Cavka, S. Jakobsen, U. Olsbye, N. Guillou, C. Lamberti, S. Bordiga and K. P. Lillerud, *J. Am. Chem. Soc.*, 2008, **130**, 13850–13851.

18 V. Guillerm, F. Ragon, M. Dan-Hardi, T. Devic, M. Vishnuvarthan, B. Campo, A. Vimont, G. Clet, Q. Yang, G. Maurin, G. Férey, A. Vittadini, S. Gross and C. Serre, *Angew. Chem., Int. Ed.*, 2012, **51**, 9267–9271.

19 W. Liang, R. Babarao and D. M. D'Alessandro, *Inorg. Chem.*, 2013, **52**, 12878–12880.

20 (*a*) S. M. Cohen, *Chem. Rev.*, 2012, **112**, 970–1000; (*b*) A. Mohmeyer, A. Schaate, B. Hoppe, H. A. Schulze, T. Heinemeyer and P. Behrens, *Chem. Commun.*, 2019, **55**, 3367–3370; (*c*) Z. Yin, S. Wan, J. Yang, M. Kurmoo and M.-H. Zeng, *Coord. Chem. Rev.*, 2019, **378**, 500–512.

21 (*a*) O. Karagiaridi, W. Bury, J. E. Mondloch, J. T. Hupp and O. K. Farha, *Angew. Chem., Int. Ed.*, 2014, **53**, 4530–4540; (*b*) B. J. Burnett, P. M. Barron, C. Hu and W. Choe, *J. Am. Chem. Soc.*, 2011, **133**, 9984–9987; (*c*) T. Li, M. T. Kozlowski, E. A. Doud, M. N. Blakely and N. L. Rosi, *J. Am. Chem. Soc.*, 2013, **135**, 11688–11691.

22 M. Schulz, N. Marquardt, M. Schäfer, D. P. Warwas, S. Zailskas and A. Schaate, *Chem.–Eur. J.*, 2019, **25**, 13598–13608.

23 W. Liang, R. Babarao, T. L. Church and D. M. D'Alessandro, *Chem. Commun.*, 2015, **51**, 11286–11289.

24 C.-W. Yu, S.-H. Li, H. Zheng and J.-G. Xu, *Chin. J. Chem.*, 2007, **25**, 797–801.

25 (*a*) T. Kajiwara, H. Higashimura, M. Higuchi and S. Kitagawa, *ChemNanoMat*, 2018, **4**, 103–111; (*b*) M. Higuchi, K. Nakamura, S. Horike, Y. Hijikata, N. Yanai, T. Fukushima, J. Kim, K. Kato, M. Takata, D. Watanabe, S. Oshima and S. Kitagawa, *Angew. Chem., Int. Ed.*, 2012, **51**, 8369–8372; (*c*) G. Y. Yoo, W. R. Lee, H. Jo, J. Park, J. H. Song, K. S. Lim, D. Moon, H. Jung, J. Lim, S. S. Han, Y. Jung and C. S. Hong, *Chem.–Eur. J.*, 2016, **22**, 7444–7451.

26 M. Schulz, A. Gehl, J. Schlenkrich, H. A. Schulze, S. Zimmermann and A. Schaate, *Angew. Chem., Int. Ed.*, 2018, **57**, 12961–12965.

27 S. Murahashi and S. Horiie, *J. Am. Chem. Soc.*, 1956, **78**, 4816–4817.

28 M. Juribašić Kulcsár, I. Halasz, A. Budimir, K. Užarević, S. Lukin, A. Monas, F. Emmerling, J. Plavec and M. Ćurić, *Inorg. Chem.*, 2017, **56**, 5342–5351.